JOURNAL OF VIROLOGY, Oct. 1999, p. 8503–8511 Vol. 73, No. 10
0022-538X/99/$04.00+0

Anterograde Transport of Herpes Simplex Virus Proteins in Axons of Peripheral Human Fetal Neurons: an Immunoelectron Microscopy Study

DAVID J. HOLLAND,[1] MONICA MIRANDA-SAKSENA,[1] ROSS A. BOADLE,[1,2] PATRICIA ARMATI,[3] AND ANTHONY L. CUNNINGHAM[1]*

Centre for Virus Research, Westmead Institutes of Health Research, Westmead Hospital and University of Sydney,[1] and Westmead Institutes of Health Research and Electron Microscope Laboratory, Westmead Hospital,[2] Westmead, New South Wales 2145, and School of Biological Sciences, University of Sydney, New South Wales 2006,[3] Australia

Received 30 April 1999/Accepted 8 July 1999

Herpes simplex virus (HSV) reactivates from latency in the neurons of dorsal root ganglia (DRG) and is subsequently transported anterogradely along the axon to be shed at the skin or mucosa. Although we have previously shown that only unenveloped nucleocapsids are present in axons during anterograde transport, the mode of transport of tegument proteins and glycoproteins is not known. We used a two-chamber culture model with human fetal DRG cultivated in an inner chamber, allowing axons to grow out and penetrate an agarose barrier and interact with autologous epidermal cells in the outer chamber. After HSV infection of the DRG, anterograde transport of viral components could be examined in the axons in the outer chamber at different time points by electron and immunoelectron microscopy (IEM). In the axons, unenveloped nucleocapsids or focal collections of gold immunolabel for nucleocapsid (VP5) and/or tegument (VP16) were detected. VP5 and VP16 usually colocalized in both scanning and transmission IEM. In contrast, immunolabel for glycoproteins gB, gC, and gD was diffusely distributed in axons and was rarely associated with VP5 or VP16. In longitudinal sections of axons, immunolabel for glycoprotein was arrayed along the membranes of axonal vesicles. These findings provide evidence that in DRG axons, virus nucleocapsids coated with tegument proteins are transported separately from glycoproteins and suggest that final assembly of enveloped virus occurs at the axon terminus.

Herpes simplex virus (HSV) normally infects two primary cell types in humans—epidermal cells (ECs) and neurons of the dorsal root ganglia (DRG). Infection usually commences with inoculation of the mucosa or epidermis, and after the virus has gained entry to axonal termini it is transported retrogradely along the axon to the neuronal cell body, where it becomes latent. Thereafter, it may reactivate in response to a number of stimuli and is transported anterogradely along the axon from the cell body to the epidermis (anterograde axonal transport) (24). The events which follow reactivation of HSV in the neuron and the process of axonal transport are not well understood. One difficulty in studying the axonal transport of HSV has been the lack of a satisfactory animal experimental model and the difficulty in obtaining and culturing human tissue (25). Cook and Stevens (5) showed that after primary infection in mice, HSV was retrogradely transported in axons as nonenveloped nucleocapsids (NC). This was confirmed by Lycke et al. in in vitro experiments with rat DRG neurons (11, 12). Anterograde axonal transport is more difficult to study because the timing of virus reactivation and transport is almost impossible to predict in animal models. Lycke et al., using cultured rat neurons, studied the anterograde transport of virus into the neurites and found enveloped virus in the soma and neurites but did not characterize transport in the primary axon (13).

Our laboratory has developed a human fetal neuron-EC model to study the anterograde axonal transport of HSV in vitro (19). Fetal DRG explants are cultured in an inner chamber (IC) from which axons grow out and penetrate a silicon agarose barrier to terminate on autologous ECs in an outer chamber (OC) (20). This system allows selective virus inoculation of the DRG in the IC and observation of viral transport along axons to the ECs. We have previously reported that HSV is present in enveloped and unenveloped forms in the neuronal soma but is transported anterogradely in axons only as nonenveloped nucleocapsids with an estimated speed of 3 to 4 mm/h (19). This rate is consistent with movement by the physiologic process of fast axonal transport associated with microtubules (17). Glycoproteins were also transported at a similar velocity and were visualized in the axon by silver-enhanced immunogold staining and scanning immunoelectron microscopy (SIEM). However, this technique was not able to resolve the relationship of glycoproteins to axonal structures or whether virus can exit from the mid-region of axons. Furthermore, these observations raise several important questions. What is the composition of the virus particle during axonal transport? Specifically, are tegument proteins associated with the nucleocapsid or with glycoprotein, or do they travel separately from both? How are the envelope glycoproteins transported? What is the site of final assembly and egress of the virus?

In this study the first two questions were addressed. Our strategy was first to validate the sensitivity and specificity of the complementary techniques of SIEM and freeze substitution transmission IEM (TIEM) for detection and spatial localiza-

* Corresponding author. Mailing address: Centre for Virus Research, Westmead Institutes of Health Research, Westmead Hospital and University of Sydney, Westmead, New South Wales 2145, Australia. Phone: (61) 2 9845 6229. Fax: (61) 2 9845 8300. E-mail: tonyc@westgate.wh.usyd.edu.au.

tion of viral antigens in infected MRC-5 cells. We then used high-magnification SIEM to examine considerable lengths of over 200 axons and assess the overall distribution of viral antigens. These findings were compared with those for similar cultures examined by TIEM, which is best suited to study short lengths of axons in detail for the localization of viral antigens to the capsid, each other, and axonal structures such as vesicles. We found that capsid and tegument proteins were colocalized and associated with particles which morphologically resembled nucleocapsids. However, glycoproteins were almost always localized separately and associated with axonal vesicles. This evidence indicates that there is separate anterograde axonal transport of the nucleocapsid and glycoproteins.

MATERIALS AND METHODS

Viruses, antibodies, and media. (i) Viruses. A clinical isolate of HSV-1 (CW1) from a patient with recurrent herpes labialis was passaged four times in MRC-5 cells (CSL, Melbourne, Australia) and typed with fluorescein-conjugated anti-gC-1 type-specific monoclonal antibody (Syva).

(ii) Antibodies. Monoclonal antibody (LP1) specific to the tegument protein VP16 was kindly provided by A. Minson, Cambridge University (15). Rabbit polyclonal monospecific antibodies to the viral capsid protein VP5 (NC1) and glycoproteins gD, gC, and gB were provided by G. Cohen and R. Eisenberg, University of Pennsylvania (4). Commercially available monoclonal antibodies to glycoprotein gB, gD, and gC were obtained from the Goodwin Institute for Clinical Research.

(iii) Media. Medium A consisted of minimal essential medium (MEM) with D-valine modification (Sigma) and supplemented with 5.12 g of glucose per liter 4% (vol/vol) Monomed (CSL), 200 mM glutamine, 20 ng of rat nerve growth factor (Collaborative Sciences) per ml, 15 μg of gentamicin per ml, and 50 μg of vancomycin per ml. Medium B consisted of MEM supplemented with 9% fetal calf serum (Gibco), 1 μg of epidermal growth factor (Sigma) per ml, 30 ng of nerve growth factor per ml, 15 μg of gentamicin per ml, and 50 μg of vancomycin per ml.

Control cell lines. MRC-5 cells (CSL), a human embryonic lung fibroblast cell line, were seeded onto coverslips. When confluent, the cells were infected with HSV-1 at a ratio of 1 to 10 PFU per cell. When cytopathic effect developed, the cells were fixed and processed for examination by transmission electron microscopy (TEM), SIEM, or TIEM as for the DRG-EC model (see below). Noninfected cells were used as controls.

DRG-EC model. (i) Preparation of model. Approval for the research was given by the Western Sydney Area Health Service and University of Sydney Ethics Committees. Human fetal tissue of 10 to 20 weeks gestation was obtained from therapeutic terminations following the informed consent of the mother.

The experimental model was a modification of that described by Penfold et al. (19, 20). Briefly, the DRG and a specimen of skin were dissected, washed, cleaned of connective tissue, and placed in medium at 4°C until explanted. The skin was cut into 1- to 2-mm^2 pieces. Stainless steel rings 1 cm in internal diameter and 1 cm high with a wall thickness of 1 mm were attached by with sterile silicon grease to Thermanox plastic coverslips (Nunc), previously coated with extracellular matrix, and placed into tissue clusterwell plates. The plates were then sterilized by microwave irradiation. On the inferior surface of the rings, a notch approximately 1 to 2 mm wide and 1 mm high was present. A sterile 2% (wt/vol) solution of low-melting-point agarose (Bio-Rad Laboratories) in double-distilled water (DDW) was pipetted inside the ring and allowed to solidify. A heated metal probe was then used to melt the center of the agarose, which was aspirated to produce an annulus of agarose on the inside of the steel ring, completing a seal between the IC and OC. The DRG were explanted into the IC, and the skin was explanted in the OC directly opposite the notch. The explants attached to the coverslip after 2 to 3 min of air drying, and then medium A was added to the IC and medium B was added to the OC (Fig. 1). The preparation was then incubated at 37°C in an atmosphere of 5% CO_2 in air.

(ii) Time course of culture. Axons arranged in fascicles grew from the DRG explant, penetrated the agarose barrier, and terminated on the ECs by 7 to 10 days. Media in both chambers were carefully aspirated; the medium in the OC was replaced with MEM plus 1% fetal calf serum and 1.5% low-viscosity carboxymethylcellulose (Sigma) immediately before 100 μl of medium A containing 2×10^3 PFU of HSV-1 was added to the IC, and most of the medium in the IC was aspirated carefully 2 h later. In experiments performed to investigate the time to emergence of virus in the OC, no carboxymethylcellulose was added to the medium. Positive controls had virus added to both chambers in the absence of the barrier. Negative controls had medium A alone added to the IC. In all experiments, duplicate 100-μl aliquots were collected from the OC 2 to 4 h after virus addition to the IC and were inoculated into MRC-5 cell cultures; experiments in which virus was isolated at this time point were not used. Up to 48 h following IC inoculation, 100-μl aliquots were collected from both the IC and OC for virus isolation, and the preparation was then fixed before removal of the ring and agarose.

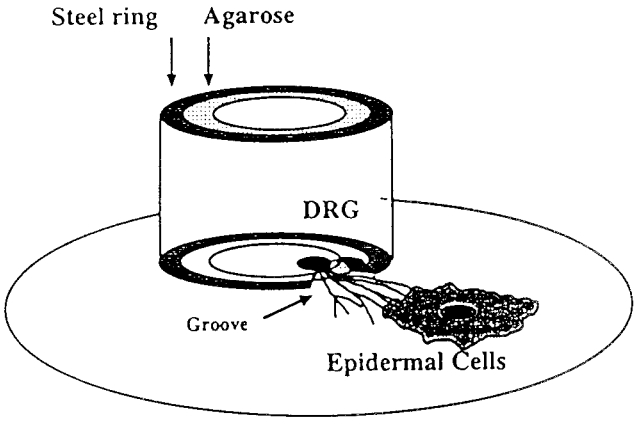

FIG. 1. Diagram of the experimental DRG-EC model. Axons usually reach the ECs by 7 to 10 days of culture, at which time virus is selectively inoculated into the inner chamber. Reprinted from reference 9 with permission from the Royal Microscopical Society.

Fixation and preparation for EM. (i) TEM. Specimens were placed in modified Karnovsky's fixative for 1 h, washed with 0.1 M morpholinepropanesulfonic acid (MOPS) buffer, and postfixed in 2% buffered osmium tetroxide for 1 h followed by 2% aqueous uranyl acetate (Fluka) for 1 h, dehydrated in graded ethanols, and infiltrated and embedded in Spurr epoxy resin (Agar Aids). Polymerization took place at 70°C for 10 h. The coverslip was detached by rapid cooling with liquid nitrogen. Ultrathin serial sections (70 nm) were double stained with 2% uranyl acetate in 50% ethanol (15 min) followed by Reynold's lead citrate solution (5 min). Sections were examined with a Philips CM10 transmission electron microscope at 80 kV.

(ii) SIEM. After being washed gently in phosphate-buffered saline (PBS), preparations were fixed in 25% acetic acid–75% methanol (vol/vol) for 8 min to permeabilize membranes as described by Penfold et al. (19), washed again three times in PBS, incubated with 5% goat serum in PBS–0.1% bovine serum albumin (BSA) for 20 to 30 min, washed twice in PBS, and then incubated for 60 min with one (single labelling) or two (double labelling) primary antibodies to the capsid protein VP5 (1:1,000 dilution), tegument protein VP16 (1:500), or glycoproteins gC, gD, and gB (1:500 to 1:1,000) diluted in PBS–0.1% BSA. Coverslips were washed three times in PBS before incubation for 60 min with the secondary antibodies, goat anti-mouse and/or goat anti-rabbit (1:50 dilution) conjugated with 10-, 20-, or 30-nm gold particles (BioCell), followed by three washes. Preparations were dehydrated in graded ethanols, critical point dried from liquid CO_2, sputter coated with a 2-nm layer of platinum, and examined in a JEOL 6500 field emission scanning electron microscope by secondary and backscatter electron modes at an accelerating voltage of 20 kV.

(iii) TIEM. Preparations were fixed in 4% formaldehyde (freshly prepared from paraformaldehyde)–0.1% glutaraldehyde for 1 h and then washed with PBS. The coverslip was trimmed to approximately 10 by 3 mm, encompassing the area of interest, coated with a thin layer of 10% gelatin which was allowed to solidify at 4°C, and then placed in cryoprotectant (1.84 M sucrose containing 20% polyvinylpyrrolidone) overnight (27). Preparations were then frozen by being rapidly plunged into liquid nitrogen and then transferred to dry methanol at −90°C in a Reichert AFS freeze-substitution system (Leica) for 40 h. The temperature was then raised to −45°C (5°C/h), and the specimens were rinsed in dry methanol and infiltrated with Lowicryl HM20 resin (Taab Laboratories). Mixtures of methanol and HM20 were used at ratios of 1:1 and 1:2 for 2 h each at −45°C followed by pure resin overnight. Embedding in HM20 was carried out with the Reichert flowthrough capsule system with polymerization by UV light at −45°C for 48 h (18). The resin block, which retained the tissue, was removed from the coverslip and reembedded in HM20 resin as before. The removal of the coverslip and reembedding (9) allowed the collection of serial ultrathin sections (70 nm) onto Formvar-Pioloform-coated grids and efficient immunolabelling. Antibodies were diluted in Tris buffer (20 mM Tris, 150 mM NaCl, 1 mg of BSA per ml, 0.05% Tween, 20 mM sodium azide) at pH 8.1, and washes were carried out in buffer at pH 7.4. Tissue sections were incubated with 5% goat serum in buffer for 30 min, washed three times for 5 min each, and incubated with the primary antibody for 2 h; the primary antibody was rabbit polyclonal anti-VP5 (1:50 dilution), mouse monoclonal anti-VP16 (1:20), or one of the antibodies to viral glycoproteins (1:20 to 1:50). The sections were then washed five times, incubated for 1 h with the secondary antibody (1:50 dilution of goat anti-rabbit or anti-mouse antibody conjugated with 5- or 10-nm gold particles [Biocell]), and washed five times in buffer. For single gold labelling, the grids were washed twice in DDW and allowed to dry. For double gold labelling, the grids were incubated with 0.5% glutaraldehyde–PBS for 30 mins, washed three times in PBS, incu-

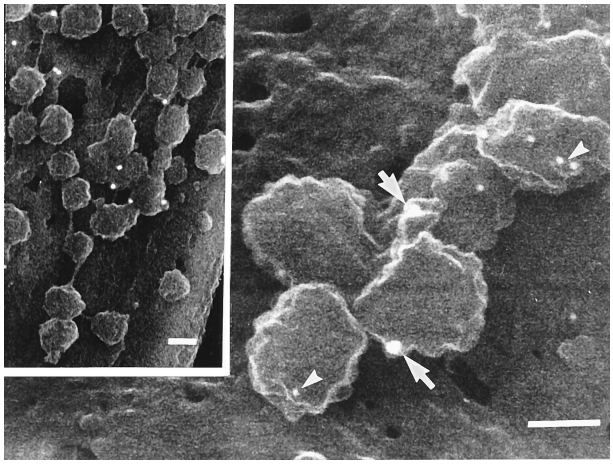

FIG. 2. SIEM of virus particles present on the surface of MRC5 cells and on neurons in the positive control of the model. The inset shows a low-magnification view of immunolabelled virions on the surface of MRC-5 cells 36 h postinfection Bar, 100 nm. The 30-nm gold particles (arrows) label gC, and the 10-nm particles (arrowheads) label VP5. Similarly immunolabelled HSV on the surface of axons in positive controls of the DRG-EC model fixed 1 h after addition of HSV is shown in the main panel. No similar virus particles were seen on the surface of axons in the OC of the infected experimental model.

bated with 0.05 M glycine–PBS for 20 min, washed three times, and incubated with a second pair of primary and secondary antibodies (as above). For each immunolabelling experiment, the order of primary antibodies and that of secondary-antibody gold size were reversed to avoid any bias due to steric hindrance.

After immunolabelling, sections were double stained with 0.5% uranyl acetate in 50% ethanol–DDW for 30 to 60 s and then with Reynolds lead citrate for 30 to 45 s. The sections were examined with a Philips CM10 transmission electron microscope at 80 kV.

RESULTS

IEM of uninfected and infected MRC-5 cells. (i) Immunolabelling of viral proteins in control MRC-5 cells by SIEM. Both infected and uninfected MRC-5 cells were examined by SIEM for HSV and immunolabel for capsid VP5, tegument VP16, and glycoprotein gC antigens. Numerous virions approximately 120 to 150 nm in diameter, with intact envelopes, were seen on or exiting from the cell membrane (Fig. 2, inset). Similar structures were not seen on uninfected cells. Permeabilization of membranes allowed immunolabelling for the submembranous proteins VP5 (capsid) and VP16 (tegument) as well as the membrane glycoproteins. Alternative methods of fixation and permeabilization of the membrane with 0.1 to 0.5% glutaraldehyde or 4% paraformaldehyde–0.1% glutaraldehyde with 0.1 to 0.5% Triton X-100 (results not shown) showed inferior results to the acetic acid-methanol method. Dual immunogold labelling recognizing VP5, VP16, and glycoproteins in paired comparisons demonstrated colocalization of all antigens on the exiting viruses (Fig. 2). gC/VP5 or VP16 immunolabel was also present on or below the cell membrane of infected cells in areas where no virus was present on the surface. Only occasional background immunolabel was observed on noninfected cells.

(ii) Immunogold labelling of viral proteins in MRC-5 cells by TIEM. The preservation of HSV ultrastructure and protein antigenicity by freeze-substitution in Lowicryl HM20 resin was first demonstrated in infected MRC-5 cells, which were processed exactly as for the DRG-EC model. Numerous virus particles were easily identifiable in cross-sections of infected cells by their characteristic size and morphology and labelled intensely with immunogold for VP5, VP16, and gB. Labelling was specific, with a very low background level of immunogold (Fig. 3). Clear examples of viral ultrastructure demonstrating the DNA core, capsid, tegument, and envelope were present (Fig. 3A and D, inset). However, most virions were tangentially sectioned with indistinct ultrastructure but still clearly identifiable by specific immunolabel for VP5 (Fig. 3A) and/or VP16 (Fig. 3B and D) in small collections or foci. Glycoprotein labelling was distributed in a reticular pattern over and around virus particles and also over vesicular structures (Fig. 3C). There was no glycoprotein labelling over the nucleus of infected cells and no immunolabelling for any viral antigen in control noninfected MRC-5 cells.

Neuron-EC model. (i) Isolation of HSV in the OC. As previously reported, HSV replicates in the neuronal and nonneuronal support cells within the IC. However, the agarose barrier usually prevents the passage of HSV from OC to IC when tested in the presence or absence of axons penetrating the agarose barrier (15a, 19). If leaks occurred, HSV was always detectable in the OC by 4 h postinfection. Therefore, each individual culture was tested at at 4 h postinfection, and if the result was positive (<20%), it was excluded from subsequent experiments, as previously reported (15a).

When carboxymethylcellulose was present in the OC culture medium, virus was not isolated from the OC at any time, even after infection of the ECs. Therefore, in experiments to determine the emergence of virus in the outside chamber, no carboxymethylcellulose was added. At 12, 24, and 48 h, virus was isolated from the supernatant in the IC and cytopathic effect was visible in some cells in the IC by 24 h postinoculation. In the OC, virus was not isolated up to 32 h after inoculation of the IC but was isolated at 48 h. Viral proteins were detectable by immunofluorescence and SIEM in both distal axons and ECs at 16 to 32 h without virus being isolated from OC culture medium (Table 1).

(ii) TEM of infected and noninfected axons. As in previous studies, enveloped and nonenveloped virus were seen in neuronal cell bodies within the DRG explant. Examination of numerous cross-sections of the mid-regions of axons, however, showed only nonenveloped nucleocapsids. These nonenveloped nucleocapsids were almost always seen in close proximity to microtubules (>95% were within 100 nm of a microtubule). Virus particles were clearly distinguished from membranous vesicles, which can have a similar appearance, depending on the angle of the section (26). Figure 4 illustrates the differences in structure between virus (Fig. 4D to F, arrowheads) and axonal vesicles (Fig. 4A to D, arrows) formally demonstrated in negative and positive controls of the DRG-EC model. Nucleocapsids could be distinguished on the basis of size, staining density, and thicker structure of the viral capsid compared to vesicle walls and by the presence of a complex internal structure in capsids, in contrast to the homogeneously staining centres of membranous vesicles.

(iii) No virions were detected on the surface of OC axons by SIEM. The axons in the OC were examined between 20 and 32 h postinfection (Table 1). These times were selected because previous (and current) studies showed that no viral antigen was present in the OC axon fascicles until after 12 h (19). HSV antigen appeared sequentially in different axons, most probably due to the different times of infection of the neuronal soma as the virus inoculum spread through the DRG explant (reference 15a and unpublished data). Therefore, at 16 to 32 h, the earliest to late stages of axonal transport were observed in different axons. No extracellular virions were seen on the surface of the mid-region of axons, although immunogold label for viral antigens (especially surface gC) was distributed along

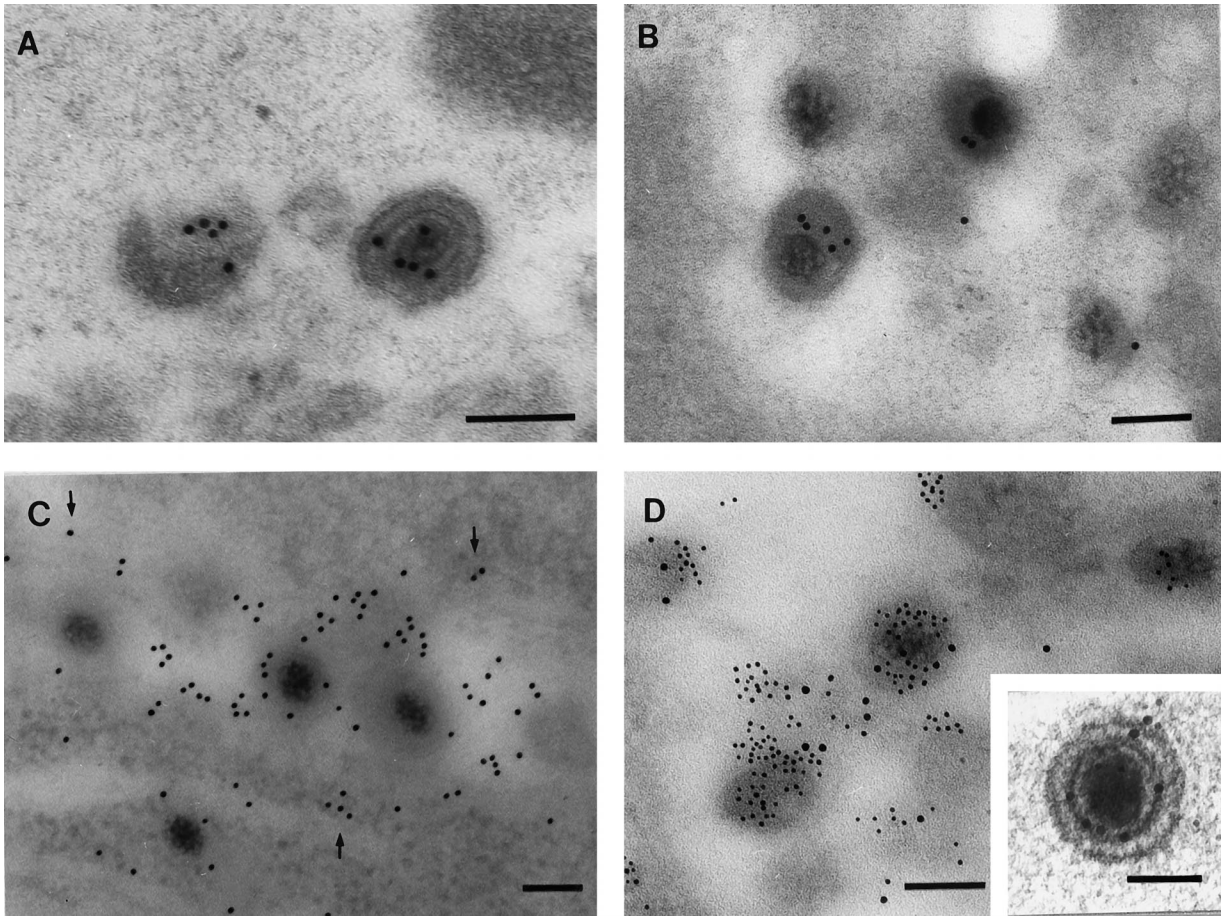

FIG. 3. TIEM of infected MRC-5 cells showing the labelling pattern for VP5, VP16, and glycoprotein, 24 h postinfection. (A) Examples of virus particles singly labeled for VP5. (B) Single labelling for VP16. (C) Single labelling for gB (10-nm particles). Note the more diffuse reticular labelling for glycoprotein over vesicular membranes (arrows) as well as virus particles. Bar, 100 nm. (D) Double labelling for VP5 (10 nm) and VP16 (5 nm). Bar, 100 nm. (Inset) High-magnification view of VP5 and VP16 double labelling of a virus with clear definition of ultrastructural morphology. Bar, 100 nm.

the axon length (see below). In positive controls, when HSV was added to both chambers, virions were clearly visible on the surface of axons and adjacent cells (Fig. 2); in noninfected controls no virus-like structures were seen and only occasional background immunolabel was observed.

(iv) Localization of immunolabel for VP5, VP16, and glycoproteins in OC axons by SIEM. Immunogold label for the capsid protein VP5 was usually distributed in small foci along the axons (Fig. 5A). Immunogold label for VP16, like VP5, was distributed in foci along the axons but was also diffusely distributed as single immunolabels at much lower density. In double-labelling experiments when counts were taken from 10 randomly selected axons, VP5 and VP16 immunolabel were colocalized within 150 nm of each other in discrete foci along the axons for >95% of VP5 antigens and for 72% of VP16 antigens. These results suggested there was an excess of VP16 antigens unassociated with VP5 (or nucleocapsids) (Fig. 5A).

Compared to the focal distribution of the immunolabel for VP5, immunolabel for glycoproteins was diffusely distributed. In contrast to the foci of colocalization of VP5 and VP16, VP5 and glycoprotein gold labels were quite separate, with fewer than 5% of VP5 immunolabel being within 150 nm of a single glycoprotein label (Fig. 5B). Furthermore, no colocalization of VP16 and glycoprotein immunolabel was observed (similar to Fig. 5B) (data not shown).

(v) Localization of immunolabel for VP5, VP16, and glycoproteins in OC axons by TIEM. Light aldehyde fixation followed by freeze substitution and embedding in Lowicryl HM20 resin was used to enhance antigenicity for immunolabelling (9). As expected, ultrastructural preservation of axon morphology was inferior to that of tissue prepared for conventional TEM (as shown by comparing Fig. 6 and 7). Microtubules were not as well visualized, especially in transverse sections, and the axoplasm generally appeared diffusely electron dense. The in-

TABLE 1. Detection of viral antigen by immunofluorescence microscopy or IEM in axons and epidermal cells and isolation of virus in supernatants from the outside chamber

Time (h) after HSV infection (in IC)	Axons in OC[a]		Epidermal cells[a]		HSV isolation from supernatants ($TCID_{50}$/ml)[a]	
	IEM	IF	IEM	IF	OC	IC
12	−	−	0	−	−	+ ($<10^2$)
16	+	+	−	−	−	+
28	++	++	+	+	−	+ (10^2–10^3)
32	++	++	++	++	−	+
48	++	++	++	++	+ (10^2–10^3)	+ (10^4–10^5)

[a] 0, not performed; +, present (++, greater extent and intensity); −, absent; IF = immunofluorescence; $TCID_{50}$, 50% tissue culture infective dose.

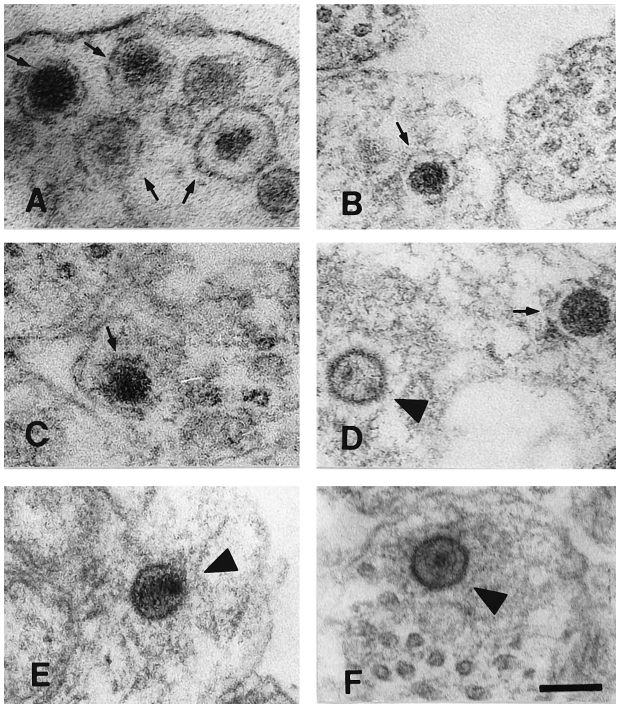

FIG. 4. TEM of axons in the infected (D to F) or noninfected (A to C) model at 24 h postinfection. The morphology of virus in tangential sections and membranous vesicles can overlap, making distinction difficult. (A to C) Membranous vesicles in a noninfected axon (arrows). (D) Both a membranous vesicle (arrow) and a nucleocapsid (arrowhead). (E and F) Viral nucleocapsids in the infected model (arrowheads). Note the close association of capsid with microtubules in panel F. Bar, 100 nm.

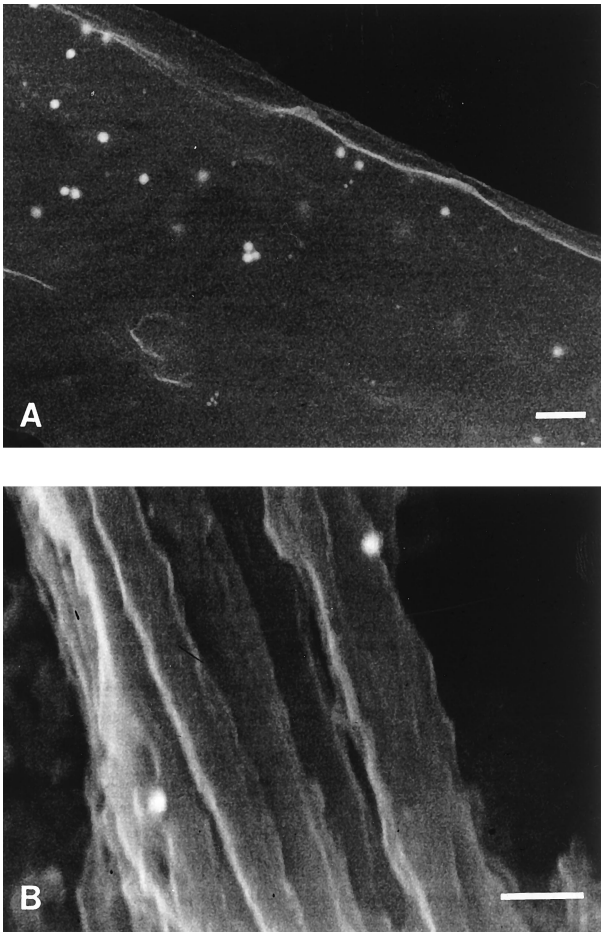

FIG. 5. SIEM of the mid-region of axons in the OC of the model, fixed 24 h after virus was inoculated into the IC. (A) Colocalization of 10-nm immunogold labelling VP5 and 20-nm immunogold labelling VP16. The 10- and 20-nm labels are intermingled within 150 nm of each other. Bar, 100 nm. (B) Dually labelled axons for VP5 and gC, but showing only the 30-nm immunolabel for gC since there was no colocalization with the 10-nm immunogold label for VP5. In fact, immunolabels for VP5 and glycoproteins could not usually be observed in the same high-power field. Note the small diameter of some axon fascicles. Bar, 100 nm.

fected model was fixed at 12 and 24 h after inoculation of the IC. At 12 h, no immunolabel recognizing viral antigens was present in cross-sections of axons. This lack of immunolabelling was the same as with noninfected controls. At 24 h postinfection, virions were identified by foci of gold immunolabel for VP5 and/or VP16. As in positive-control axons, clear examples of virus ultrastructure associated with specific immunolabel for viral proteins were encountered only rarely and depended on a fortuitous angle of section through the center of the virus (Fig. 7D and F). Most commonly, virus was tangentially sectioned, resulting in indistinct morphology, but was identified by dense and specific label for VP5 (Fig. 7A and B) or VP16. Immunolabel for VP5 and VP16 were intermingled in some of these foci (Fig. 7A). Furthermore, when clusters of VP5 and VP16 immunolabel were observed in the same section (10 in 2,000 sections examined), they always colocalized within 100 nm of each other. However, single VP16 immunolabels were sparsely distributed and unassociated with VP5. In some cases, an ultrathin section (70 nm) clearly demonstrated a virus capsid. Serial sections immediately before and after these sections demonstrated no obvious virus structure but did show immunolabel for VP5 or VP16.

In longitudinal sections of axons, labelled virions were observed in apposition to microtubules. VP16 label was also found diffusely and lightly distributed in the axon independent of VP5 label (results not shown). Overall, this pattern of immunolabelling was consistent with that observed by SIEM and with the location of nucleocapsids by TEM (Fig. 4D to F).

In contrast to the colocalization of VP5 and VP16, neither gC, gD, nor gB colocalized with VP5 (Fig. 7B to D) or VP16 (Fig. 7F), a pattern similar to that observed by SIEM; i.e., <5% of clusters of immunolabel for gC or gD were observed within 150 nm of VP5 (or VP16). Rather, immunolabel for glycoproteins was diffusely distributed in cross-sections and longitudinal sections of the axon. Immunogold label for gC or gB was often seen in small collections, which were separate to foci of capsid or tegument label (Fig. 7B to E). In longitudinal sections and cross-sections, immunolabel for gC or gB was arrayed along the walls of vesicles ranging between 60 and 200 nm in diameter (Fig. 7E).

Single gC or gB immunolabel was rarely observed (<5%) within 50 nm of the surface of the dense-cored nucleocapsids which were immunolabelled for VP5 or VP16.

DISCUSSION

In our previous work with the DRG-EC model and conventional TEM, we found only unenveloped nucleocapsids in axons, whereas both enveloped and unenveloped virions were present in the soma of neurons (19). Rapid transport of both capsid (VP5) and glycoprotein antigen at ~3 to 4 mm/h was demonstrated by serial fixation, immunofluorescence, and con-

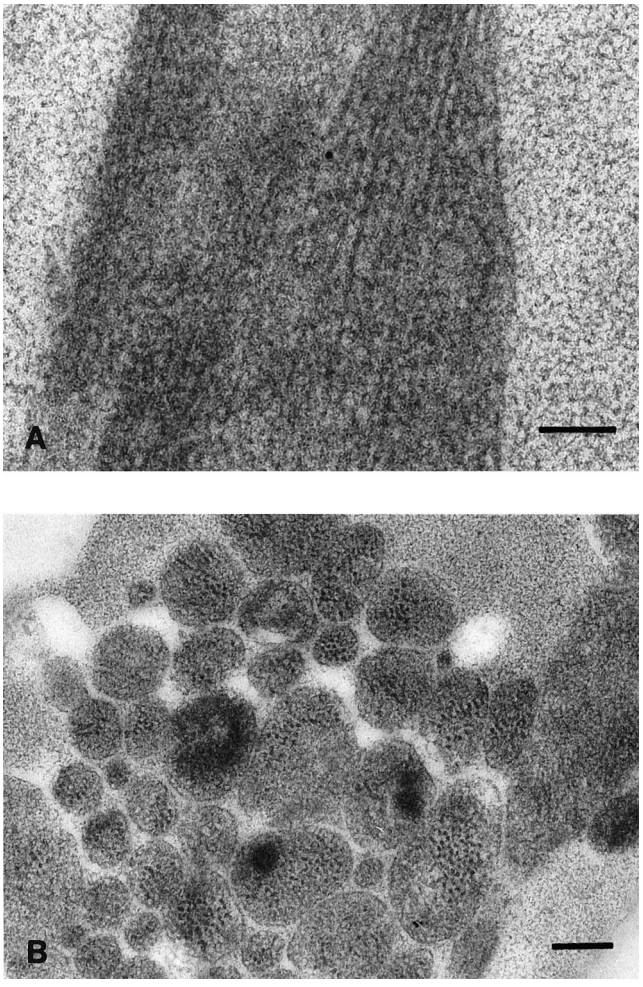

FIG. 6. TEM of axons. Longitudinal (A) and transverse (B) sections of axons in OC are shown. Microtubules are easily visible in the longitudinal sections and in some axons in the transverse sections. Bar, 200 nm.

focal microscopy. SIEM with silver enhancement of permeabilized axons showed the presence but not the location of glycoprotein antigen, below and on the axonal membrane, raising the possibility that virus exits from the mid-region of the axon. Overall, these findings suggested that there was separate anterograde axonal transport of nucleocapsids and glycoproteins.

The present study used both high-magnification SIEM and TIEM without silver enhancement to identify and localize virions, nucleocapsids, and antigens within axons and their association with axonal structures. The association of the tegument protein VP16 with the capsid and localization of the separate transport of glycoproteins in vesicles was demonstrated. This protein is a major constituent of all layers of the tegument (14, 22, 34). In addition, the present study did not detect any virus exiting from the mid-region of the axon or of extracellular infectious HSV before transmission to the epidermis, suggesting that virus assembles and exits further distally, from the axon terminus.

Using SIEM, we were able to examine considerable lengths of axon at high magnification and assess the overall distribution of antigen. However, to examine the distribution of viral antigens and their relationship to each other and to structures within the axon, we developed a technique of freeze substitution-TIEM, applicable to cultures on coverslips (9).

With SIEM, focal collections of capsid (VP5) and tegument (VP16) antigens were shown to mostly colocalize (70% were found within 150 nm, the diameter of a virion with attached antibodies). In other regions of the axon, VP16 antigen was separate from capsid immunolabel in a sparse, diffuse distribution. Colocalization of VP5 and glycoprotein or of VP16 and glycoprotein antigens was rare (<5% of VP5 or VP16 was within 150 nm of glycoprotein). This was not due to relative lack of avidity of the glycoprotein antibodies, as shown by approximately equal labelling of virus with all three antibodies in infected MRC5 cells. However, colocalization of all classes of antigen, VP5, VP16, and glycoproteins and a greater density of all immunolabel was observed at the axon terminus by SIEM (9a).

TIEM provided corroborative data allowing positive identification of virions as foci of immunolabel for nucleocapsid (VP5) and tegument (VP16) antigens with adequate preservation of axonal ultrastructure. In contrast, the colocalization of VP5 and glycoprotein antigens was rare. Rather, glycoprotein antigen was seen in groups or in linear arrays and along the walls of 60- to 200-nm-diameter vesicles. This observation is consistent with the expected transport site of these proteins, which have hydrophobic transmembrane segments. Both in TEM and in longitudinal sections in TIEM, nucleocapsids or foci of VP5 and/or VP16 antigen were in close proximity to microtubules. Although glycoprotein antigens were observed on the surface of the axons by SIEM, no virions were seen exiting or on the surface of the mid-axon region. However, exiting virions were easily visible and demonstrated colocalization of all classes of antigens in the positive controls of infected MRC-5 cells. Virions were also observed in the DRG-EC model, where HSV was directly added to cells or axons. These findings were consistent with the absence of infectious virions in the extracellular fluid of the OC until 32 to 48 h after inoculation of virus into the IC.

The ability of SIEM and TIEM to identify virus particles and antigens was central to this study and was checked exhaustively in infected and uninfected MRC-5 cells and in control uninfected and infected DRG-EC cultures.

Freeze-substitution processing for TIEM (9, 18, 27) was shown in infected MRC5 cells to preserve antigenicity of the virus (Fig. 3), allowing double labelling and eliminating the need for silver enhancement, which obscures labelling and the underlying structure. The specificity of immunolabelling was demonstrated by the presence of foci of label over viral structures and membranes and the lack of label in other areas of the cell or in noninfected MRC-5 cells or axons. VP5 immunolabel was confined to the nucleus at early stages of infection of MRC5 cells, but glycoprotein label was never observed over the nucleus. Freeze substitution was chosen as a technique which preserved antigenicity but which also could be adapted to process delicate structures retained on coverslips (9). However, a drawback of preservation of antigenicity was the variable preservation of the ultrastructural detail of axons (compared to conventional TEM). Microtubular and vesicular structures were not as clearly visible, especially in transverse section, and the axoplasm was more homogeneously electron dense. Nevertheless, the localization of immunolabelled antigen to viral and axonal structures could still be demonstrated. In sections of MRC-5 cells, approximately 90 to 95% of virions showed indistinct morphology, since most were cut tangentially, but were identifiable because of foci of immunolabel for VP5 or VP16. Since it can be difficult to distinguish nucleocapsids from some axonal vesicles in conventional TEM (26), we found immunoelectron microscopy to be the most reliable method for identifying HSV virions and proteins in axons.

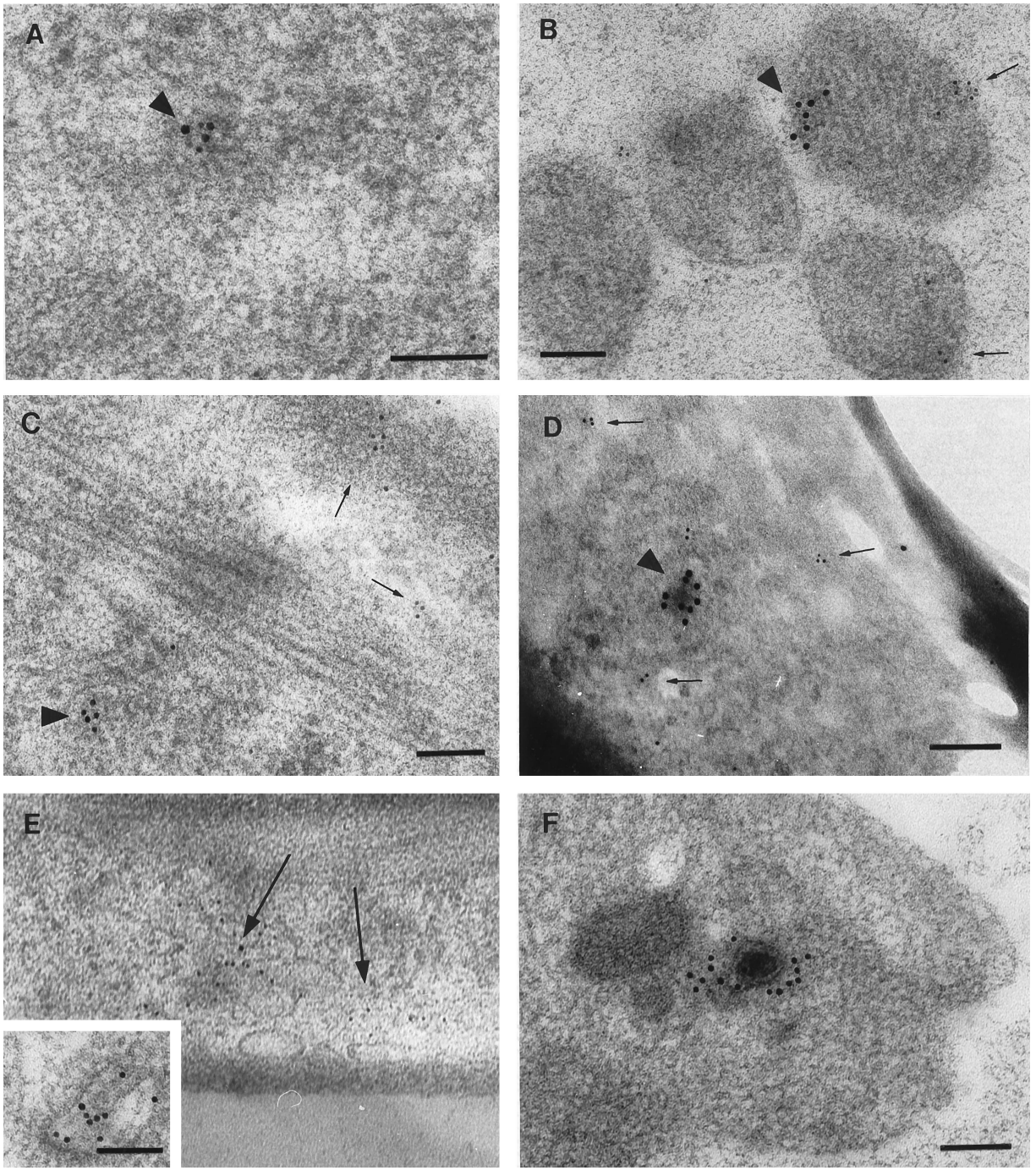

FIG. 7. TIEM of axons in the outside chamber of the model fixed 24 h after HSV infection of the inner chamber. Bars, 100 nm. (A) Colocalization of gold particles labelling VP5 (10 nm) and VP16 (5 nm) in a cluster. (B and C) Spatial separation of collections of immunolabel for VP5 (10 nm; arrowheads) and glycoprotein C (5 nm; arrows) in a cross section (B) and longitudinal section (C) of axons. (D) Similar pattern to panels B and C with double labelling for VP5 (10 nm) and glycoprotein B (5 nm); the immunolabel for VP5 was arranged around a dense structure, and that for gB was arranged around microvesicles. Identical findings were obtained with immunolabelling for gD. (E) Immunolabel for gB 5-nm gold particles was arrayed around the walls of 60- to 200-mm-diameter vesicles. The inset shows a higher-magnification view of glycoprotein immunolabelling of an axonal vesicle. Bar, 100 nm. (F) Distinct example of a nucleocapsid with immunolabel (10 nm) for VP16. Although this section was also immunolabelled for glycoprotein, none is present near this capsid. Ultrathin sections immediately before and after this section showed only indistinct virus structures.

It is unlikely that the nucleocapsid or tegument foci and free glycoprotein represent irrelevant excess virus material following transport of enveloped virions within vesicles down the axonal fascicles. The timing of the emergence and transport of nucleocapsid and/or glycoprotein antigen in axons in the OC was previously determined by immunofluorescence and confocal microscopy and used to determine time points for SIEM and TIEM studies (19) and was recently confirmed (data not shown). No viral antigens were detected at 12 h. In addition, virus transport in each axon in the OC does not occur synchro-

nously but at different phases related to the time of infection of sensory neurons as the virus spreads through the DRG explant. However, the pattern of immunogold label was consistent in all axons, and no coassociation of VP5 and glycoproteins was seen. Complementary studies of the transport of HSV antigen in axons have also been performed with dissociated neurons, and concordant findings were obtained: anterograde transport of capsid antigen in axons peaked at 16 to 24 h after direct infection of dissociated neurons. No antigen was present in axons at 12 h. Treatment of neurons with nocodozole, a depolymerizer of microtubules, blocked rapid anterograde transport of nucleocapsid and glycoproteins.

Furthermore, treatment with brefeldin A, which causes fusion of Golgi and endoplasmic reticulum membranes, resulted in dissociation of anterograde VP5 and glycoprotein transport (15b). These studies showed that anterograde transport of VP5 antigen and/or intact nucleocapsids by TIEM was not inhibited by brefeldin A, while glycoprotein transport was completely abrogated.

Therefore this combined data strongly argues for separate anterograde axonal transport of glycoproteins transported with conventional membrane vesicles and nucleocapsids probably conveyed by a direct interaction with microtubular motor proteins. Immunolabelling studies examining a possible colocalization of viral components with conventional kinesins, the microtubule-associated motor proteins responsible for anterograde transport of organelles (28, 29, 30, 32), are in progress.

Our findings have relevance for hypotheses about the egress of herpesviruses from cells (1–3, 6–8, 10, 16, 22, 23, 31). After capsid assembly in the nucleus and budding through the inner nuclear membrane into the perinuclear space, two alternative pathways are possible: suggested; (i) the enveloped particles enter a transport vesicle derived from the outer membrane and are transported to the Golgi and then via the endoplasmic reticulum to the cell surface by exocytosis (2, 24), or (ii) the enveloped particles are deenveloped at the outer nuclear membrane (accounting for the large number of unenveloped nucleocapsids in the cytoplasm), enveloped in or close to the Golgi, and then exocytosed (1, 16, 21, 22, 31). The first hypothesis suggests that final tegumentation occurs wholly in the nucleus, whereas in the second at least some tegumentation could occur in the cytoplasm. Our results show that the deenveloped virions present in the cytoplasm are functional and not "dead-end" as suggested by the first hypothesis. They are capable of being transported separately from glycoproteins along the axon and assembled into virions. We have recently shown increased density and convergence of HSV glycoprotein, tegument, and nucleocapsid antigens at the axon terminus, which supports a process of distal assembly (9a).

Thus, HSV is transported within axons both in anterograde and retrograde directions as unenveloped nucleocapsids, in contrast to transport in the cell body, which occurs as enveloped virions 150 nm in diameter within vesicles, at least from the Golgi to the cell surface. This suggests that there is a biological advantage in transport of unenveloped nucleocapsids over long distances. Furthermore, since sensory axons may be as small as 100 to 200 nm in diameter, there may be an advantage to the separate transport of viral subcomponents along small-diameter axons, with final assembly occurring at the axon terminus. The process of anterograde axonal transport described above may also be relevant to other neurotropic viruses transported along axons, such as varicella zoster virus pseudorabies virus, and rabies virus.

ACKNOWLEDGMENTS

This work was supported by an Australian National Health and Medical Research Grant (no. 970738) and by an NHMRC postgraduate scholarship to David Holland.

We thank Gary Cohen and Ros Eisenberg for antibodies to VP5, gB, gC, and gD; Tony Minson for LP1 monoclonal antibody; The University of Sydney Electron Microscope Unit for access to and assistance with field emission SEM; Carol Robinson, Gayle Avis, and Levina Dear from the ICPMR/WIHR EM laboratory for providing valuable photographic assistance; and Mark Penfold for help with the model. Our thanks to Brenda Wilson for typing the manuscript.

REFERENCES

1. **Browne, H., S. Bell, T. Minson, and D. W. Wilson.** 1996. An endoplasmic reticulum-retained herpes simplex virus glycoprotein H is absent from secreted virions: evidence for reenvelopment during egress. J. Virol. **70:**4311–4316.
2. **Campadelli-Fiume, G., F. Farabegoli, S. Di Gaeta, and B. Roizman.** 1991. Origin of unenveloped capsids in the cytoplasm of cells infected with herpes simplex virus 1. J. Virol. **65:**1589–1595.
3. **Cheung, P., B. W. Banfield, and F. Tufaro.** 1991. Brefeldin A arrests the maturation and egress of herpes simplex virus particles during infection. J. Virol. **65:**1893–1904.
4. **Cohen, G. H., M. Ponce de Leon, H. Diggelmann, W. C. Lawrence, S. K. Vernon, and R. J. Eisenberg.** 1980. Structural analysis of the capsid polypeptides of herpes simplex virus types 1 and 2. J. Virol. **34:**521–531.
5. **Cook, M. L., and J. G. Stevens.** 1973. Pathogenesis of herpetic neuritis and ganglionitis in mice: evidence for intra-axonal transport of infection. Infect. Immun. **7:**272–288.
6. **Eggers, M., E. Bogner, B. Agricola, H. F. Kern, and K. Radsak.** 1992. Inhibition of human cytomegalovirus maturation by brefeldin A. J. Gen. Virol. **73:**2679–2692.
7. **Granzow, H., F. Weiland, A. Jons, B. G. Dlupp, A. Karger, and T. C. Mettenleiter.** 1997. Ultrastructural analysis of the replication cycle of pseudorabies virus in cell culture: a reassessment. J. Virol. **71:**2072–2082.
8. **Harson, R., and C. Grose.** 1995. Egress of varicella-zoster virus from the melanoma cell: a tropism for the melanocyte. J. Virol. **69:**4994–5010.
9. **Holland, D., A. L. Cunningham, and R. A. Boadle.** 1998. The axonal transmission of Herpes simplex virus to epidermal cells: a novel use of the freeze substitution technique applied to explant cultures retained on coverslips. J. Microsc. **192:**69–72.

9a. **Holland, D., et al.** Unpublished data.

10. **Jones, F., and C. Grose.** 1988. Role of cytoplasmic vacuoles in varicella-zoster virus glycoprotein trafficking and virion envelopment. J. Virol. **62:**2701–2711.
11. **Kristensson, K., E. Lycke, M. Roytta, B. Svennerholm, and A. Vahlne.** 1986. Neuritic transport of herpes simplex virus in rat sensory neurons in vitro. Effects of substances interacting with microtubular function and axonal flow (nocodazole, taxol and erythro-9-3-(2-hydroxynonyl)adenine). J. Gen. Virol. **67:**2023–2028.
12. **Lycke, E., K. Kristennsson, B. Svennerholm, A. Vahlne, and R. Ziegler.** 1984. Uptake and transport of herpes simplex virus in neurites of rat dorsal root ganglia cells in culture. J. Gen. Virol. **65:**55–64.
13. **Lycke, E., B. Hamark, M. Johansson, A. Krotochwil, J. Lycke, and B. Svennerholm.** 1988. Herpes simplex virus infection of the human sensory neuron: an electron microscopy study. Arch. Virol. **101:**87–104.
14. **McLaughlin, J., and F. J. Rixon.** 1992. Characterization of enveloped tegument structures (L particles) produced by alphaherpesviruses: integrity of the tegument does not depend on the presence of capsid or envelope. J. Gen. Virol. **73:**269–276.
15. **McLean, C., A. Buckmaster, D. Hancock, A. Buchan, A. Fuller, and A. Minson.** 1982. Monoclonal antibodies to three non-glycosylated antigens of herpes simplex virus type 2. J. Gen. Virol. **63:**297–305.

15a. **Mikloska, Z., P. P. Sanna, and A. L. Cunningham.** Neutralizing antibodies inhibit axonal spread of herpes simplex virus type 1 to epidermal cells in vitro. J. Virol. **73:**5934–5944.

15b. **Miranda-Saksena, M., et al.** Submitted for publication.

16. **Nii, S., C. Morgan, and H. M. Rose.** 1968. Electron microscopy of herpes simplex virus. II. Sequence of development. J. Virol. **2:**517–536.
17. **Ochs, S., and W. S. Brimijoin.** 1993. Axonal transport, p. 331–360. *In* P. J. Dyck, P. K. Thomas, J. W. Griffin, P. A. Low, and J. F. Podeslo (ed.), Peripheral neuropathy, 3rd ed. The W. B. Saunders Co., Philadelphia, Pa.
18. **Oprins, A. D., H. J. Geuze, and J. W. Slot.** 1994. Cryosubstitution dehydration of aldehyde fixed tissue: a favourable approach to quantitative immunocytochemistry. J. Histochem. Cytochem. **42:**497–503.
19. **Penfold, M. E. T., P. Armati, and A. L. Cunningham.** 1994. Axonal transport of herpes simplex virions to epidermal cells: evidence for a specialized mode of virus transport and assembly. Proc. Natl. Acad. Sci. USA **91:**6529–6533.
20. **Penfold, M. E., P. J. Armati, Z. Mikloska, and A. L. Cunningham.** 1996. The

interaction of human fetal neurons and epidermal cells in vitro. In Vitro Cell Dev. Biol. Anim. **32:**420–426.
21. **Rixon, F. J., C. Addison, and J. McLauchlan.** 1992. Assembly of enveloped tegument structures (L particles) can occur independently of virion maturation in herpes simplex virus type 1-infected cells. J. Gen. Virol. **73:**277–284.
22. **Rixon, F. J.** 1993. Structure and assembly of herpesviruses. Semin. Virol. **4:**135–144.
23. **Roffman, E., J. P. Albert, J. P. Goff, and N. Frenkel.** 1990. Putative site for the acquisition of human herpesvirus 6 virion tegument. J. Virol. **64:**6308–6313.
24. **Roizman, B., and A. E. Sears.** 1996. Herpes simplex viruses and their replication, p. 2231–2295. *In* B. N. Fields, D. M. Knipe, P. M. Howley, et al. (ed.), Fields virology, 3rd ed. Lippencott Raven, Philadelphia, Pa.
25. **Stanberry, L. R.** 1992. Pathogenesis of herpes simplex virus infection and animal models for its study. Curr. Top. Microbiol. Immunol. **179:**15–30.
26. **Thomas, P. K., C.-H. Berthold, and J. Ochoa.** 1993. Microscopic anatomy of the peripheral nervous system, p. 28–91. *In* P. K. Thomas, P. J. Dyck, J. Poduslo, P. A. Low, and J. Griffin (ed.), Peripheral neuropathy, 3rd ed. The W. B. Saunders Co., Philadelphia, Pa.
27. **Tokuyasu, K. T.** 1989. Use of poly(vinylpyrrolidone) and poly(vinyl alcohol) for cryoultramicrotomy. Histochem. J. **21:**163–171.
28. **Vale, R. D., T. S. Reese, and M. S. Sheetz.** 1985. Identification of a novel force-generating protein, kinesin, involved in microtubule-based motility. Cell **42:**39–50.
29. **Vale, R. D., B. J. Schnapp, T. Mitchison, E. Steuer, T. S. Reese, and M. P. Sheetz.** 1985. Different axoplasmic proteins generate movement in opposite directions along microtubules *in vitro*. Cell **43:**623–632.
30. **Vallee, R. B., and M. P. Sheetz.** 1996. Targeting of motor proteins. Science **271:**1539–1544.
31. **Whealy, M. E., J. P. Card, R. P. Meade, A. K. Robbins, and L. W. Enquist.** 1991. Effect of brefeldin A on alphaherpesvirus membrane protein glycosylation and virus egress. J. Virol. **65:**1066–1081.
32. **Yamazaki, H., T. Nakata, O. Yasushi, and N. Hirokawa.** 1995. KIF3A/B: a heterodimeric kinesin superfamily protein that works as a microtubule plus end-directed motor for membrane organelle transport. J. Cell Biol. **130:**1387–1399.
33. **Zhu, Q., and R. J. Courtney.** 1994. Chemical cross-linking of virion envelope and tegument proteins of herpes simplex virus type 1. Virology **204:**590–599.
34. **Zhu, Z., M. D. Gershon, C. Gabel, D. Sherman, R. Ambron, and A. Gershon.** 1995. Entry and egress of varicella-zoster virus: role of mannose 6-phosphate, heparan sulfate proteoglycan, and signal sequences in targeting virions and viral glycoproteins. Neurology **45:**S15–S17.